Cornichon regulates transport and secretion of TGFα-related proteins in metazoan cells

Carolina Perez Castro, Denise Piscopo, Takatoshi Nakagawa and Rik Derynck*

Department of Cell and Tissue Biology, Program in Cell Biology, University of California at San Francisco, San Francisco, CA 94143-0512, USA
*Author for correspondence (e-mail: rik.derynck@ucsf.edu)

Accepted 11 May 2007
Journal of Cell Science 120, 2454-2466 Published by The Company of Biologists 2007
doi:10.1242/jcs.004200

Summary

Cornichon proteins are structurally related transmembrane proteins that have been studied in and *Drosophila* and yeast. In *Drosophila*, Cornichon (Cni) is involved in embryo polarization by the TGFα-related Gurken. In yeast, the Cni-related Erv14 is required for axial budding. A cargo receptor function has been proposed for Erv14 and Cni. Four mammalian Cni-like sequences have been identified. We carried out parallel functional analyses of the human Cni ortholog CNIH and *Drosophila* Cni in the processing and presentation of TGFα family proteins. Human CNIH complements the loss of Erv14 in yeast. Human CNIH and *Drosophila* Cni are primarily localized in the endoplasmic reticulum and associate with immature TGFα family proteins. Alterations of cornichon expression result in changes in transport, processing and secretion of TGFα proteins. In particular, increased cornichon expression retains TGFα proteins in the endoplasmic reticulum, whereas cornichon is required for their transport and secretion. Thus, cornichon proteins represent a functionally conserved protein family that acts in the selective transport and maturation of TGFα family proteins.

Key words: Cornichon, EGFR, Transport, Secretion, Functional conversation

Introduction

Transforming growth factor α (TGFα) and related proteins are ligands for the epidermal growth factor receptor (EGFR) in metazoans ranging from *Drosophila* and *C. elegans* to mammals, and they activate a signaling pathway that affects numerous cell fate decisions. Aberrant EGFR activation or expression is involved in cell transformation, tumor progression and metastasis of cells from neuroectodermal origin and has been implicated in the initiation and progression of human cancer (Derynck, 1992; Lee et al., 1995; Schlessinger, 2002). Although the signaling events initiated by EGFR activation are well described, further insight into the mechanisms of ligand processing, transport and secretion is essential to understand the regulation and deregulation of ligand-induced EGFR signaling in normal development and cancer.

TGFα family proteins, including Spitz and Gurken (Grk) in *Drosophila*, are made as type I transmembrane proteins with an extracellular six-cysteine containing EGF core domain. This EGF domain is essential for receptor binding and activation. Proteolytic shedding removes the ectodomain to generate soluble ligand. Thus, TGFα proteins function both as transmembrane ligands and as soluble ligands that can act at a distance (Derynck, 1992; Massague and Pandiella, 1993). In mammalian cells, TGFα undergoes processing and maturation during its transport through the secretory pathway. Following synthesis and removal of the signal peptide, the 20 kDa immature TGFα form is transported from the endoplasmic reticulum (ER) to the Golgi, most likely via COPII-mediated vesicular transport. Concomitantly, TGFα is glycosylated, resulting in a heterogeneous population in the 30 kDa range, as determined by SDS-PAGE, a reflection of the inherent heterogeneity of N-glycosylation (Bringman et al., 1987; Fan and Derynck, 1999). Regulated proteolytic cleavage targets the TGFα ectodomain, thereby releasing the N-glycosylated prosequence and generating a 15 kDa transmembrane TGFα form and soluble TGFα ligand that contains the EGF core domain (Brachmann et al., 1989; Massague and Pandiella, 1993). The generation of soluble TGFα is activated by MAP kinase pathways and is, in the case of growth factor- or phorbol ester (PMA)-induced shedding, mediated by the metalloprotease tumor necrosis factor α converting enzyme (TACE) (Fan and Derynck, 1999; Sunnarborg et al., 2002). Ectodomain shedding is generally upregulated in tumor cells (Derynck, 1992), probably as a consequence of enhanced MAP kinase signaling (Fan and Derynck, 1999). The mechanisms that regulate TGFα transport from the ER to the Golgi, and from the Golgi to the plasma membrane, as well as the processing of the ligand by ectodomain shedding, are not well defined.

In addition to its role in cell proliferation, ligand-activated EGFR signaling is involved in cell differentiation and development (Shilo, 2005). The role of EGFR signaling in development has been best defined in model systems such as *Drosophila* (Perrimon and Perkins, 1997; Ray and Schupbach, 1996; Schweitzer et al., 1995) and *C. elegans* (Hopper et al., 2000). The genetic accessibility of *Drosophila* has allowed the identification of ligands that activate EGFR, as well as proteins that are required for presentation of the ligands to the receptor (Neuman-Silberberg and Schupbach, 1996; Tsruya et al., 2002; Urban et al., 2002). One EGFR ligand in *Drosophila* is Grk, which is processed to release soluble Grk, similar to TGFα and other TGFα family proteins. Ligand-induced EGFR activation by Grk requires

three other proteins that play key roles in transport and maturation, Cornichon (Cni) (Bokel et al., 2006; Roth et al., 1995), Rhomboid (Guichard et al., 2000; Urban et al., 2002) and Star (Ghiglione et al., 2002; Urban et al., 2002). Mutations in *Cni* confer developmental phenotypes that resemble those caused by inactivation of the genes encoding Grk or EGFR (Roth et al., 1995).

Cni is a 16 kDa protein with three transmembrane domains. A Cni homolog in yeast, called Erv14, is required for axial budding of daughter cells and has been proposed to serve as a cargo receptor, based on its requirement for transport of Axl2 to the site of bud selection (Powers and Barlowe, 1998). This requirement, together with the localization of Erv14 to the ER and its ability to interact in vitro with COPII, led to the proposal that Erv14 is a component of COPII-coated vesicles that mediate cargo export from the ER (Powers and Barlowe, 2002). The idea that Cni may have a similar function in transporting Grk in *Drosophila* is supported by the recently reported interaction of a segment of Grk with Cni in vitro and the requirement for Cni in Grk-induced EGFR activation in *Drosophila* oocyte development (Bokel et al., 2006). There have been no reports that homologs of Cni, Rhomboid or Star are involved in the transport and processing of vertebrate TGFα family proteins.

We now provide evidence that cornichon proteins have similar functions in mammalian and *Drosophila* cells, consistent with their structural conservation. Specifically, we focused on the regulatory role of cornichon proteins during transport and processing of EGFR ligands. Our findings indicate that cornichon proteins are functionally conserved in yeast, *Drosophila* and mammalian cells. Furthermore, we show that in metazoans cornichon proteins have a similar subcellular localization and regulate transport of TGFα family ligands.

Results

Cornichon is evolutionarily conserved

A full-length human cornichon [CNIH; cornichon homolog (Drosophila)] cDNA was obtained by PCR using the *Drosophila* Cni cDNA (NM_165151) sequence for primer design. The cloned sequence corresponds to the 144-amino acid cornichon-like isoform 1, TGAM7 (Utku et al., 1999). Four CNIH sequences have been reported in GenBank (cornichon-like isoform 1, accession number NP_005767; cornichon homolog 2, accession number NP_872359; cornichon homolog 3, accession number NP_689708; cornichon homolog 4, accession number NP_054903). These four paralogs share substantial identity throughout their entire polypeptide sequence (Fig. 1A).

Comparison of the CNIH sequence to orthologs in mouse, *Drosophila* and yeast (Fig. 1B; data not shown) reveals substantial sequence conservation, suggesting a potentially conserved role in function. Erv14, Cni and CNIH proteins have three predicted transmembrane segments, indicative of a multimembrane spanning topology (Powers and Barlowe, 2002). The loop between the first and second transmembrane domains contains three acidic residues that are conserved in all cornichon proteins. As proposed for Erv14 (Powers and Barlowe, 2002), this loop is expected to face the lumen of the ER, whereas the segment between the second and third transmembrane regions would be exposed to the cytosol.

Subcellular localization of cornichon proteins

The sequence conservation of mammalian CNIH and *Drosophila* Cni, in comparison with yeast Erv14, raises the question of whether all three proteins have a similar subcellular localization. In yeast, Erv14 localizes to the ER and Golgi structures (Powers and Barlowe, 1998), whereas in *Drosophila*, Cni localizes primarily to the ER (Bokel et al., 2006). We determined the subcellular localization of tagged CNIH and Cni in human HeLa and *Drosophila* S2 cells, respectively (Fig. 2). In HeLa cells, CNIH was shown by immunofluorescence to localize to the perinuclear region in a diffuse reticular pattern, characteristic of the ER and coincident with staining for calnexin, a marker of the ER (Fig. 2A). CNIH can also be seen to localize to discrete punctae, some of which colocalize with calnexin. The immunofluorescence for tagged CNIH showed partial overlap with GM130, a Golgi marker (Fig. 2B), indicating localization of CNIH in the Golgi. The staining for both calnexin and GM130 was similar in non-transfected cells and cells expressing CNIH. CNIH also colocalized partially with endogenous SEC23, a component of the COPII vesicle coat complex that localizes to ER exit sites, in HeLa cells (Fig. 2E). Identical localization was observed independent of whether the proteins were Myc-, Flag- or HA-tagged (data not shown). We also determined the subcellular localization of endogenous CNIH in HeLa cells. We raised an antiserum to the conserved peptide from amino acid 32-46 of CNIH (Fig. 1) and used it to detect CNIH in HeLa cells, which express CNIH as determined by RT-PCR (data not shown). The staining for endogenous CNIH (Fig. 2C) was similar to that of HA-tagged CNIH in transfected cells, albeit with lower intensity (Fig. 2A).

In S2 cells, tagged Cni showed a similar perinuclear and reticular cytoplasmic staining (Fig. 2F) as in HeLa cells (Fig. 2A-E). The staining of Cni showed significant overlap with that of KDEL-GFP, which localizes to the ER (Fig. 2F). The localization of Cni-Myc overlapped partially with that of the Golgi marker p120 (Fig. 2G). No CNIH or Cni staining was detected at the cell surface in either HeLa or S2 cells (Fig. 2, data not shown).

To more precisely define the subcellular localization of Cni, we performed immunoelectron microscopy on Cni-Myc-expressing S2 cells. The anti-Myc staining was specific, with 91% of the membrane-associated immunostaining associated with the ER (Fig. 2I, arrowheads, and Table 1). Double labeling was performed using an antibody against Sec23 (also known as dSec23p), the *Drosophila* homolog of SEC23, which localizes to ER exit sites (Kondylis and Rabouille, 2003). Approximately a quarter (26%) of the labeled Cni-Myc colocalized with Sec23 (Fig. 2J), indicating that a fraction of Cni is in the transitional ER (Fig. 2J). The labeling density for Cni was much higher at the exit sites than in the surrounding cytosol. A small fraction of Cni, 9% of the membrane-associated labeling, was detected in Golgi stacks (data not shown), consistent with the immunofluorescence localization (Fig. 2G).

CNIH expression rescues the budding phenotype of yeast lacking Erv14

To evaluate a functional conservation of cornichon among diverse organisms, we examined whether CNIH, which is

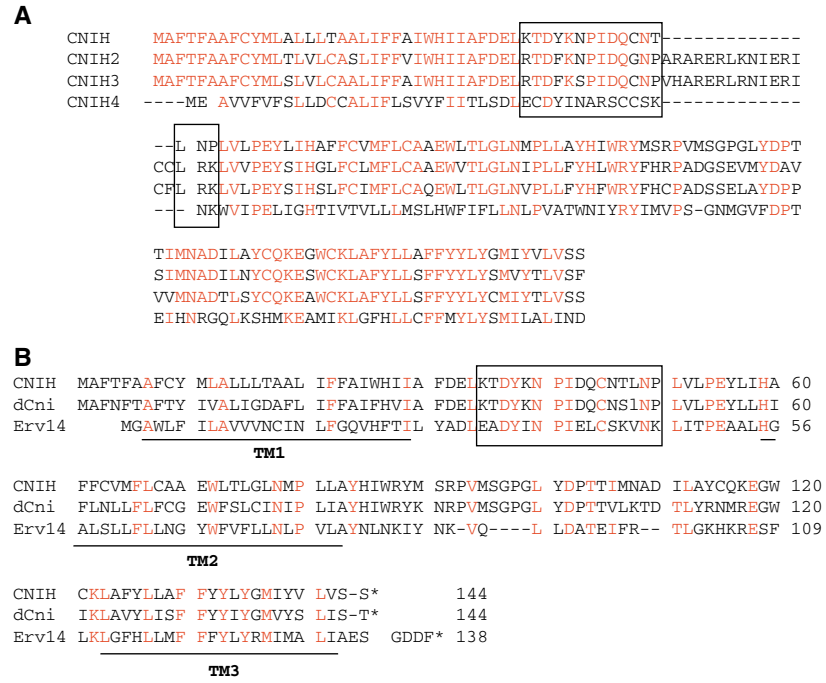

Fig. 1. Polypeptide sequences and predicted transmembrane topology for human, *Drosophila* and yeast cornichon proteins. (A) Alignment of the amino acid sequences CNIH, CNIH2, CNIH3 and CNIH4. The identity of CNIH with each of the other paralogs is: 105/159 (66%) with CNIH2; 109/160 (68%) with CNIH3; 45/118 (38%) with CNIH4. (B) Alignment of CNIH, *Drosophila* Cni (dCni) and Erv14. The identity of CNIH with each ortholog is: 96/144 (66%) with dCni and 45/137 (32%) with Erv14. Predicted transmembrane domains are underlined. The conserved 'Cni domain' is boxed. Identical residues are in red.

phylogenetically more distant from yeast Erv14 than Cni, could rescue the altered budding pattern observed in yeast with a null allele at the Erv14 locus, the erv14Δ strain (Powers and Barlowe, 1998). In contrast to the typical axial budding pattern of an isogenic wild-type strain, haploid erv14Δ yeast cells showed non-axial budding, as reported (Powers and Barlowe, 1998). Transformation of erv14Δ cells with Erv14 or HA-tagged Erv14 rescued the axial budding phenotype with high efficiency, as expected (Powers and Barlowe, 1998). Remarkably, CNIH-HA rescued the non-axial budding phenotype with 76% efficiency, compared with 79% for Erv14-HA (Table 2). This result indicates a functional conservation of CNIH and Erv14. Since axial budding is achieved by proper transit of Axl2 through the secretory pathway (Powers and Barlowe, 1998), these results strongly suggest that CNIH is able to load Axl2 into COPII vesicles at the exit from the ER and, thus, functions as a cargo receptor similar to Erv14.

Cornichon colocalizes and physically interacts with TGFα family proteins

The genetic and functional association of Erv14 with Axl2 in yeast (Powers and Barlowe, 1998), and Cni with Grk in *Drosophila* (Roth et al., 1995), prompted us to examine whether cornichon proteins physically associate with TGFα family proteins. Immunofluorescence revealed colocalization of TGFα with CNIH in transfected HeLa cells at sites where CNIH is normally present, i.e. in the ER and Golgi (Fig. 2D). Similarly, we observed colocalization of Grk with Cni in S2 cells (Fig. 2H), suggesting that both proteins interact during ligand transport and processing.

The colocalization of cornichon proteins with TGFα family proteins prompted us to examine their physical association by coimmunoprecipitation from HeLa cell extracts (Fig. 3). Among the three TGFα forms, the immature 20 kDa TGFα form (form 1), which has its prosegment but lacks full N-glycosylation, interacted most efficiently with CNIH-Myc (Fig. 3A, lane 4). However, the larger form of transmembrane TGFα (form 2), which is fully N-glycosylated in the Golgi (Bringman et al., 1987), did not co-precipitate. The preferential interaction of CNIH with immature TGFα is consistent with their colocalization in the ER. No interaction was detected when extracts of cells expressing TGFα were mixed with those of CNIH-Myc-expressing cells and subjected to coimmunoprecipitation (Fig. 3A, lane 5). In addition, the transferrin receptor, SEC61β and EGF receptor did not co-precipitate with CNIH (Fig. 3A; data not shown). However, CNIH did interact with another member of the TGFα family, amphiregulin (AR). Notably, CNIH interacted specifically with the form of AR that was shown to be the immature precursor (Fig. 3B lanes 3) (Brown et al., 1998). Furthermore, increasing CNIH expression enhanced the relative levels of immature transmembrane TGFα and AR (Fig. 3A,B), suggesting that CNIH may help retain TGFα family proteins in their immature forms. Since the structural

Table 1. Relative distribution of *Drosophila* Cni and COPII in S2 cells

Label	ER (%)	Golgi (%)
Sec23 (COPII)*	98	<2
Cni-Myc†	91	9
Cni-Myc + Sec23‡	26	ND

*As detected with 15 nm-gold particles, n=132; †as detected with 10 nm-gold particles, n=297; ‡as detected with 10 nm-gold particles associated in the same membrane with 15 nm-gold particles. Quantifications are derived from S2 cells (n=20).

Table 2. CNIH complements Erv14 function in yeast in a budding assay of haploid cells

Strain	Number of non-axial budding cells* (total)	Non-axial budding (%)
WT/pRS316	6 (108)	5.5
erv14/pRS316	81 (100)	81
erv14/pRS316-Erv14	18 (80)	22
erv14/pRS316-Erv14HA	11 (51)	21
erv14/pRS316-CNIH-HA	110 (464)	24

*Log phase cells with four or more bud scares were evaluated for non-axial budding patterns. Cells that display one or more bud scars at opposite poles were scored as non-axial.

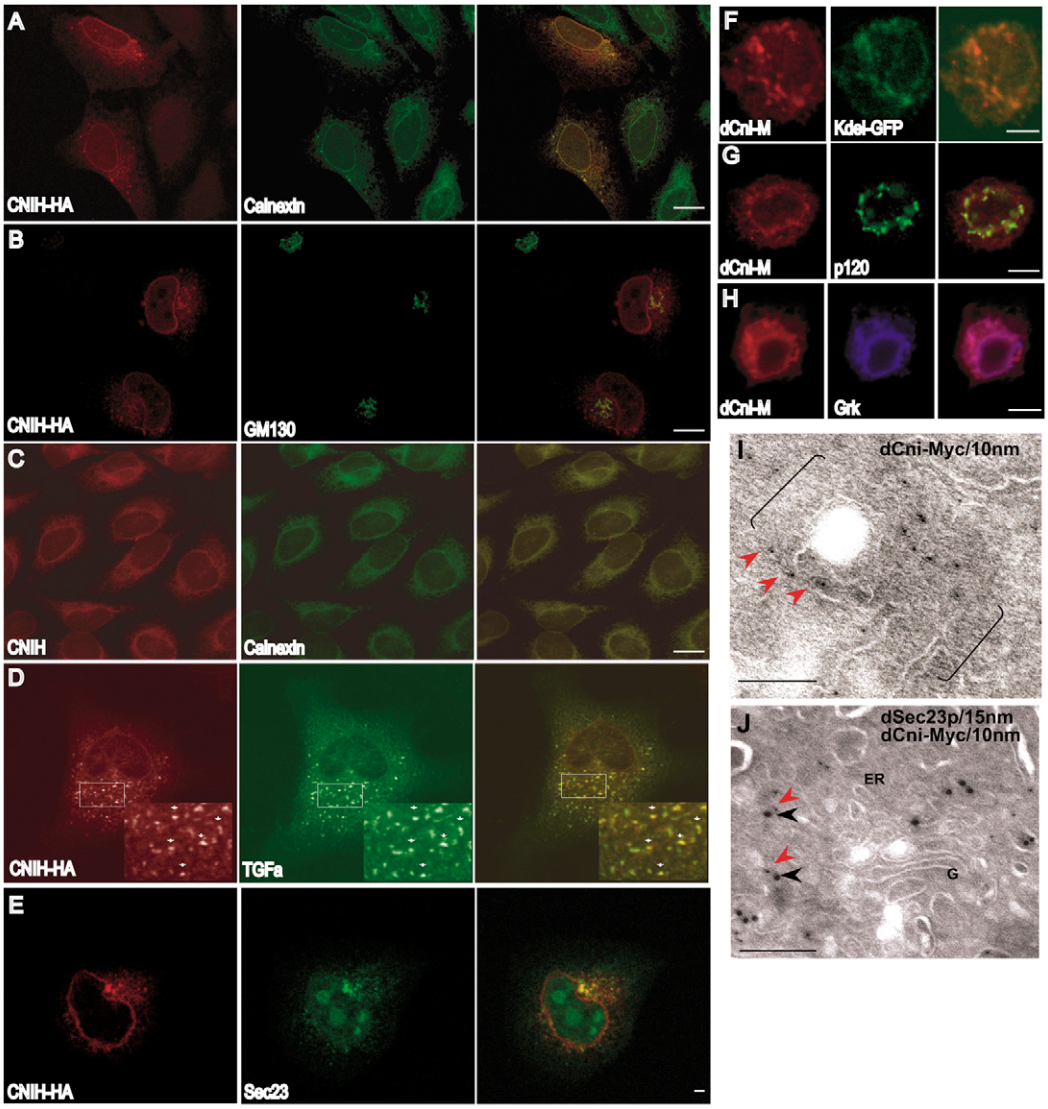

Fig. 2. Cornichon localizes in the ER and partially in the Golgi, and colocalizes with TGFα ligands. (A,B) Colocalization of HA-tagged CNIH with endogenous calnexin, a marker of the ER, and GM130, a cis-Golgi marker, in HeLa cells. HA-CNIH is only expressed in transfected cells, whereas calnexin and GM130 are expressed in all cells. Bar, 10 μm. (C) Detection of endogenous CNIH in HeLa cells and colocalization with calnexin. Bar, 10 μm. (D) Partial colocalization of CNIH and TGFα in transfected HeLa cells. (E) Partial colocalization of SEC23 (Sec23) with CNIH in HeLa cells. Bar 2 μm. (F-H) Myc-tagged *Drosophila* Cni (dCni-M) in transfected S2 cells colocalizes with the ER marker KDEL-GFP (F), partially colocalizes with the Golgi marker p120 (G), and colocalizes with ectopically expressed Grk. Bar, 10 μm (H). (I,J) Immunoelectron microscopy detection of dCni-M in S2 cells. (I) Anti-Myc antibody (10-nm gold particles) detected dCni-Myc (red arrowheads) on buds from the ER, and adjacent vesicular and tubular membranes. Brackets indicate clusters of vesicles and tubules of the ER. (J) Double immunodetection of dCni and Sec23 (dSec-23p), a COPII vesicle marker. Myc-tagged dCni (red arrowheads) and Sec23 in COPII vesicles (black arrowheads) were visualized using 10 nm and 15 nm gold particles, respectively. Bar, 200 nm.

similarity of transmembrane TGFα and AR is confined to their EGF core domains, these data suggest that CNIH interacts with TGFα family proteins that are characterized by an EGF core sequence. We also examined whether Cni-Myc coimmunoprecipitated with Grk in lysates from transfected S2 cells. This interaction, consistent with the in vitro data of Bokel et al. (Bokel et al., 2006), was more difficult to detect in comparison with the CNIH-TGFα interaction. This may be due to differences in antibody interactions or might suggest that Cni and Grk interact only weakly (Fig. 3C, lane 4).

We next evaluated which TGFα segments interact with CNIH (Fig. 3D). Deletion of the cytoplasmic domain of transmembrane TGFα (TGFαΔC) did not prevent the association with CNIH. It should be noted that the ΔC mutation itself impairs processing of TGFα (Kuo et al., 2000), resulting in accumulation of immature TGFα, as seen in the immunoblot of the lysate. By contrast, replacement of the 50-amino acid EGF core in the ectodomain with an unrelated Myc epitope tag sequence (TGFαΔE) abolished the interaction (Fig. 3D, compare lane 7 with lanes 3 and 5, upper panel). We conclude that the EGF core of transmembrane TGFα, and presumably

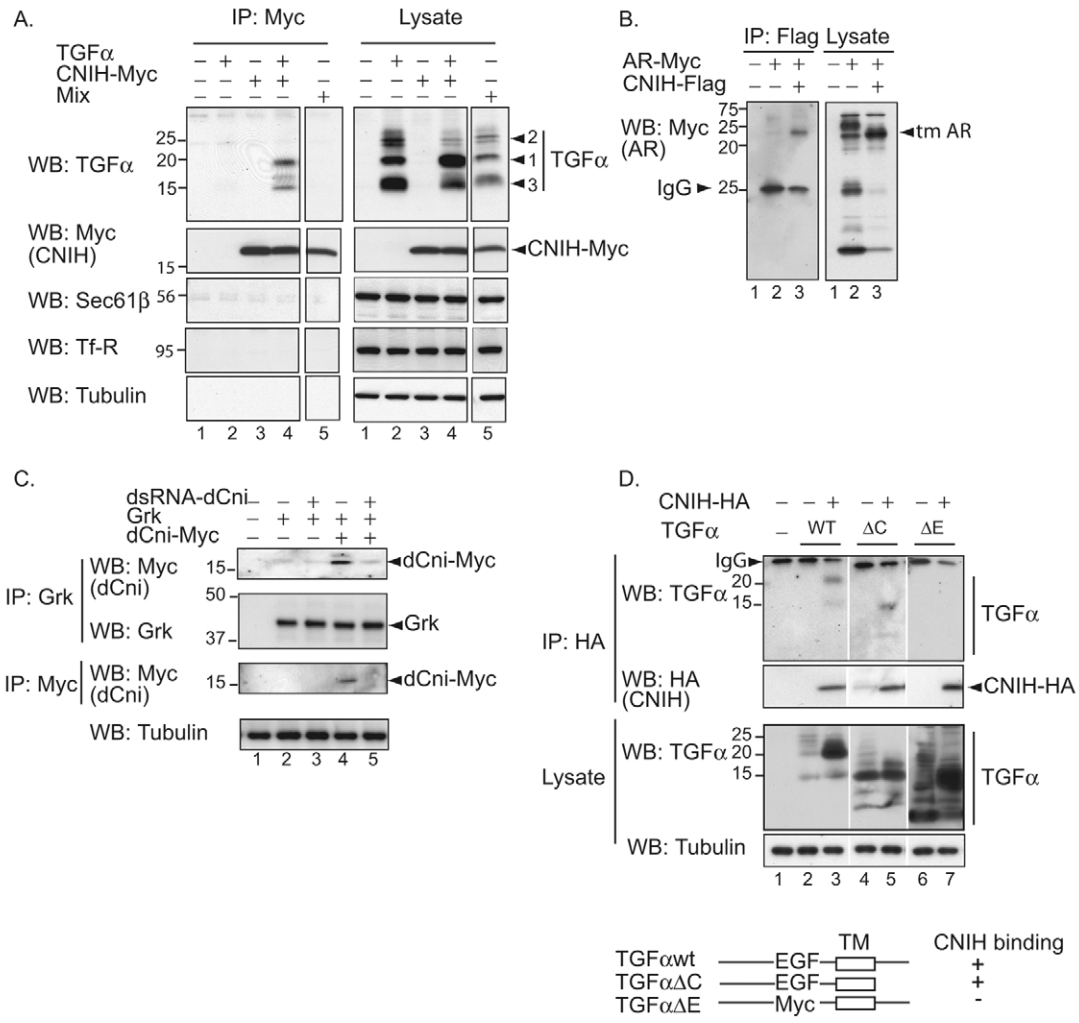

Fig. 3. Cornichon interacts with TGFα family members. (A) CNIH interacts with TGFα. Left: lysates of HeLa cells expressing TGFα and/or Myc-tagged CNIH subjected to immunoprecipitation with anti-Myc, and immunoblotting with indicated antisera. Right: total cell lysates subjected to immunoblotting. TGFα co-precitated with CNIH-Myc only when coexpressed and not when separately expressed and cell lysates were mixed (lane 5). CNIH did not interact with SEC61β (Sec61β), an ER resident protein, or transferrin receptor (Tf-R). (B) CNIH interacts with amphiregulin (AR). Left: lysates of HeLa cells expressing Myc-tagged AR and/or Flag-tagged CNIH, subjected to immunoprecipitation with anti-Flag, and immunoblotting with anti-Myc. Right: total cell lysates subjected to immunoblotting to detect AR. Immature AR is marked. (C) *Drosophila* Cni interacts with Grk. S2 cells were transfected or not transfected to express Myc-tagged dCni (dCni-Myc) and treated or not with dsRNAi targeting dCni. Lysates were processed for Grk immunoprecipitation and immunoblotting with anti-Myc or anti-Grk antibodies. dCni-Myc co-precipitated with Grk, only when Grk and dCni-Myc were coexpressed in the absence of dsRNAi targeting Cni. dsRNAi targeting Cni did not affect Grk expression. (D) The EGF core of transmembrane TGFα is required for interaction with CNIH. HeLa cells were transfected to express HA-tagged CNIH and full-length TGFα, TGFαΔC or TGFαΔE. Cell lysates were subjected to anti-HA immunoprecipitation, and immunoblotting to detect CNIH-associated TGFα. TGFα and TGFαΔC were detected using an anti-TGFα antibody Ab-1, and TGFαΔE was detected using anti-Myc. Lysates of non-transfected cells served as controls. Dividing vertical white lines indicate parts from the same gel (A,D).

of other TGFα family proteins, is required for association with CNIH.

CNIH interacts with components of the secretory pathway

In the course of our analyses, we found that CNIH co-precipitated with GM130, a cis-Golgi marker implicated in vesicle and protein transport from the ER to the cis-Golgi (Fig. 4A, lane 4). CNIH co-precipitated with GRASP55, localized in the cis/medial Golgi protein, but only in the presence of coexpressed TGFα (Fig. 4B, compare lanes 3 and 4). GRASP55 interacts with the cytoplasmic domain of TGFα and regulates its transport through the Golgi (Kuo et al., 2000). We did not find any difference in the association of TGFα and GRASP55 when CNIH was overexpressed (Fig. 4B, lanes 2 and 3). These results are consistent with the partial localization of CNIH to the Golgi and the hypothesis that CNIH cycles between the ER and Golgi. Our results also suggest the formation of multiprotein complexes that contain CNIH, GRASP55 and transmembrane TGFα, presumably in the Golgi.

Effect of CNIH on TGFα processing and transport

Since CNIH and TGFα interact and are localized to similar subcellular compartments, we evaluated the effect of increased CNIH expression on TGFα processing, transport and secretion (Fig. 5). Expression of CNIH, even at low levels, decreased the levels of the mature TGFα forms (form 2 and 3) and enhanced the level of immature 20 kDa TGFα (form 1; Fig. 5A, top panels). Coimmunoprecipitation of increasing levels of immature TGFα with CNIH (Fig. 5A, bottom panels) was also apparent. Increased CNIH expression also enhanced the level of immature endogenous TGFα in HCA-7 epithelial cells (Fig. 5B). Further, in CHO cells stably expressing TGFα, ectopic CNIH expression increased the amount of TGFα at sites were CNIH is localized, indicative of an accumulation of immature TGFα in the ER. Costaining with GM130 shows TGFα primarily localized to the Golgi in cells that do not ectopically express CNIH, but enhanced retention of TGFα in the ER in cells with ectopic CNIH expression (Fig. 5C). Semi-quantitative image analysis of the immunostaining indicated a threefold increase in intracellular accumulation of TGFα in CNIH co-transfected cells (Fig. 5D). Importantly, the accumulated immature TGFα colocalized with CNIH (Fig. 5C). Ectopic expression of Cni also increased the relative level of immature TGFα in mammalian cells (data not shown), suggesting that CNIH and Cni function similarly in TGFα processing and transport.

We next attempted to define which region of CNIH was responsible for this effect on TGFα processing. Among several CNIH deletion mutants (data not shown), only the CD1 mutant did not enhance the level of immature TGFα relative to the other two TGFα forms (Fig. 5E, compare lanes 2 and 3). The CD1 mutant has a 20-amino acid C-terminal deletion of the third transmembrane region, but remarkably runs with the same mobility as full-size CNIH in SDS-PAGE. In addition, CD1 interacted more strongly with immature TGFα than full-size CNIH. This result indicates that the C-terminal segment of CNIH is required for retention of transmembrane TGFα in its immature form, and that the efficiency of CNIH association with TGFα does not strictly correlate with retention.

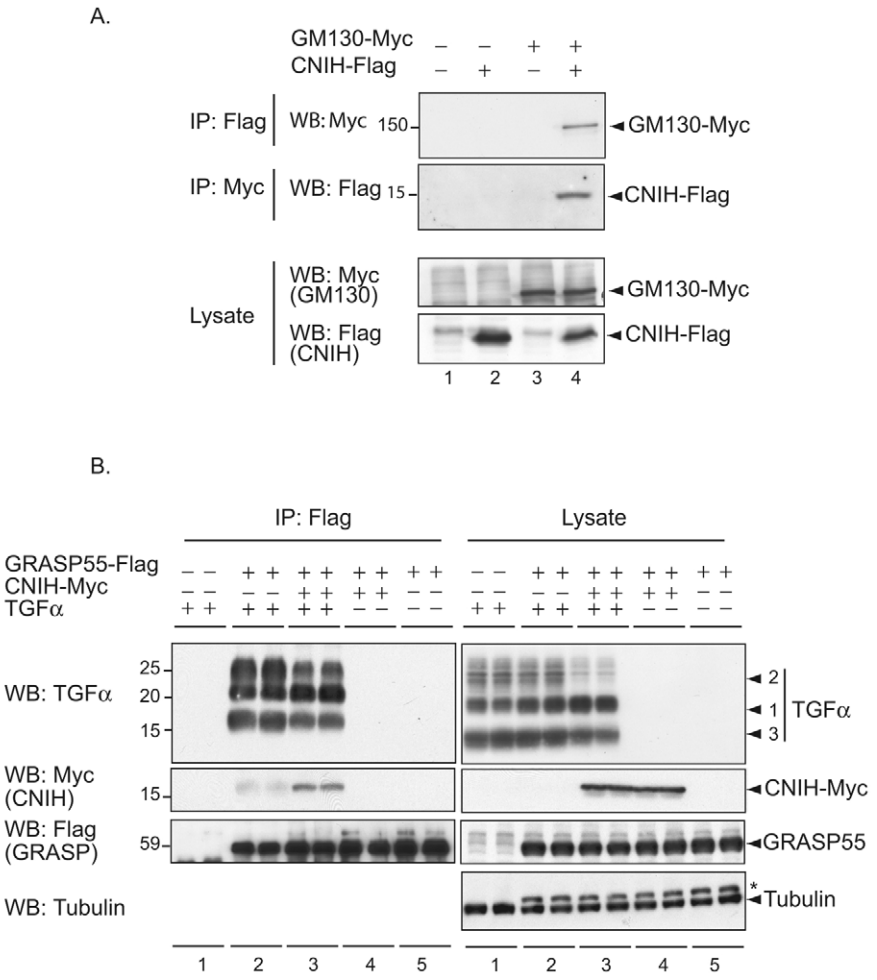

Fig. 4. CNIH interacts with proteins of the secretory pathway. (A) CNIH interacts with GM130. HeLa cells, transfected to express Myc-tagged GM130 with or without Flag-CNIH, were subjected to anti-Flag immunoprecipitation and immunoblotting with anti-Myc, or conversely with anti-Myc followed by anti-Flag immunoblotting. (B) HeLa cells, transfected to express Flag-tagged GRASP55, with or without TGFα or Myc-tagged CNIH, were subjected to anti-Flag immunoprecipitation, followed by immunoblotting for TGFα or Myc-CNIH. GRASP55 immunoprecipitated with CNIH in the presence of TGFα, but not in its absence. *Bands corresponding to a remaining GRASP55 immunoblot signal prior to tubulin immunoblotting. All samples were prepared and loaded in duplicate.

Effect of CNIH on cell surface expression and secretion of TGFα

The retention of immature TGFα in the ER with increased CNIH expression would be expected to result in a decrease in the level of mature TGFα that reaches the cell surface. To test this, we examined the surface level of TGFα in the presence of CNIH. When CNIH was ectopically expressed, the level of TGFα labeled by cell surface biotinylation was decreased with a concomitant increase in the relative level of immature TGFα in the cell lysate (Fig. 6A, compare lanes 1 and 2). CNIH did not affect the cell surface expression of gp130, a transmembrane protein that does not associate with CNIH (Fig. 6B; data not shown).

Consistent with the retention of TGFα in its immature form and the decrease in cell surface presentation of TGFα, increased CNIH expression decreased the secretion of soluble TGFα. TGFα release occurs as a result of ectodomain shedding from transmembrane TGFα following cleavage by membrane-bound metalloproteases. This release results from the activity of the metalloprotease TACE and involves activation of the p38 and/or Erk MAP kinase pathways (Fan

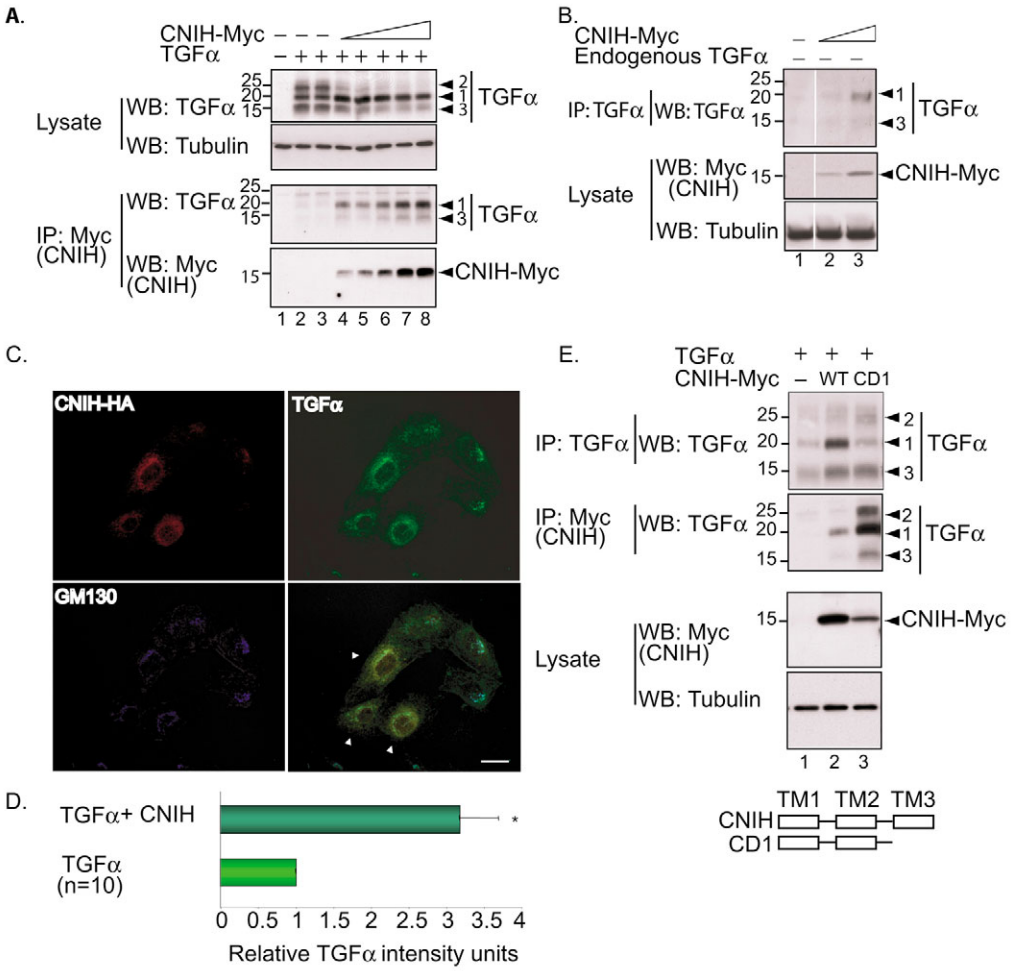

Fig. 5. Effects of CNIH on TGFα maturation. (A) CNIH increased the immature TGFα form. CHO cells were transfected to express TGFα in the presence of increasing CNIH-Myc levels. Upper panel: expression of TGFα in cell lysates, showing an increase in immature TGFα (form 1), relative to the mature forms 2 and 3. Lower panels: increased TGFα levels co-precipitated with CNIH-Myc. (B) Effect of CNIH on endogenous TGFα in HCA-7 cells. Cells were transfected to express CNIH-Myc (20 and 100 ng plasmid), and co-precipitation of endogenous TGFα with CNIH was examined. (C) Effect of CNIH-HA on TGFα localization in transfected CHO cells. In the absence of HA-CNIH, TGFα had a diffuse distribution. CNIH expression conferred TGFα accumulation in the ER, where CNIH is localized. Bar, 20 μm. (D) The Semi-quantitative image analysis of TGFα immunostaining (given as relative TGFα intensity units) shows three times more accumulation of intracellular TGFα signal in comparison with cells not transfected with CNIH. Error bars represent s.e.m.; **t*-test, $P<0.05$. (E) Comparison of full-length CNIH and CD1 deletion mutant; TM, transmembrane. Transfected cells expressed full-length or CD1 mutant CNIH-Myc and TGFα. Cell lysates were processed for anti-Myc immunoprecipitation and immunoblotting with anti-TGFα. Dividing vertical lines indicate parts from the same gel (B).

and Derynck, 1999; Sunnarborg et al., 2002). TGFα release was quantified by expressing transmembrane TGFα that is extracellularly fused to alkaline phosphatase (AP-TGFα), thus allowing the use of an enzymatic assay to measure soluble AP-TGFα (Sahin et al., 2004). When CNIH was coexpressed with AP-TGFα, the level of soluble AP-TGFα in the medium was reduced by approximately 50% (Fig. 6C). A comparable effect of CNIH on ectodomain shedding was observed with AR, similarly tagged with AP (data not shown). These results indicate that the interaction of CNIH with transmembrane TGFα family proteins decreases maturation, cell surface presentation and secretion through ectodomain shedding of these EGFR ligands.

PMA activates ectodomain shedding and, accordingly, enhanced the level of AP-TGFα in the medium. PMA also enhanced the level of released AP-TGFα in the presence of CNIH, and the relative induction of shedding was similar in the absence or presence of CNIH (Fig. 6C). Similar results were obtained when shedding of AP-fused AR was induced with PMA (data not shown). Moreover, the subcellular distribution of the metalloprotease TACE was unaffected by ectopic CNIH expression (Fig. 6D). Therefore, we conclude that CNIH expression does not affect ectodomain shedding per se.

We also compared the level of N-glycosylation of TGFα in the presence of CNIH. Treatment of TGFα with *N*-glycosidase F, which removes N-linked glycosylation proximal to Asn, increased the gel mobility of the TGFα bands (Fig. 6E, lane 2, upper panel), indicating carbohydrate removal. Coexpression of CNIH enhanced the level of immature TGFα (form 1),

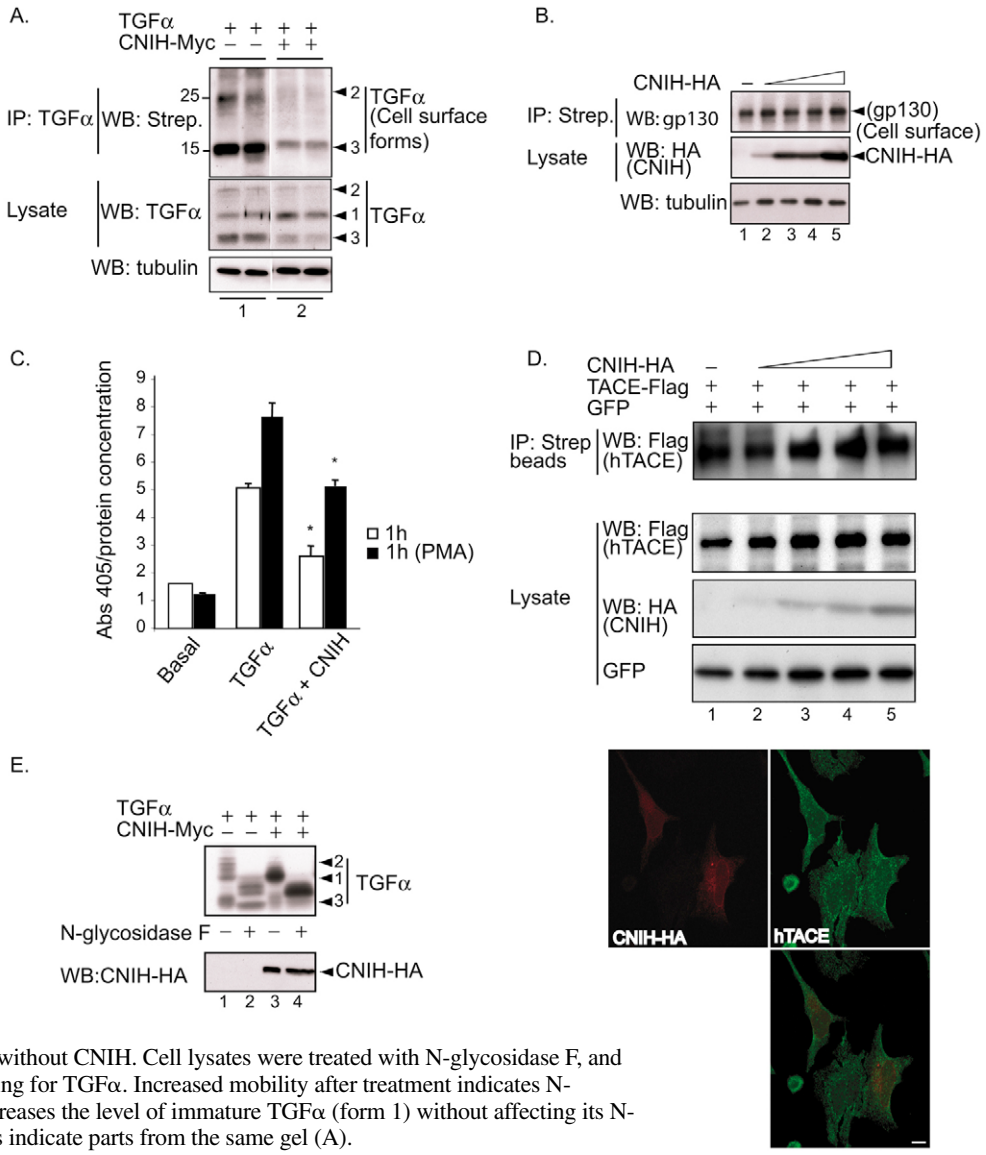

Fig. 6. Increased CNIH expression decreases the cell surface level and secretion of TGFα. (A) CNIH decreases cell surface TGFα in transfected HCA-7 cells, assessed by cell surface protein biotinylation, followed by anti-TGFα immunoprecipitation and streptavidin blotting. Duplicate samples were analyzed. Lower panel: total TGFα in cell lysates, demonstrating increased relative level of immature TGFα (form 1) in the presence of CNIH. (B) CNIH does not affect the cell surface expression of gp130, assessed by cell surface protein biotinylation, followed by avidin precipitation and anti-gp130 blotting. (C) CNIH significantly reduces the level of soluble TGFα. Secretion of AP-TGFα, measured using an alkaline phosphate assay, in the medium of HeLa cells with or without CNIH. PMA was added to activate shedding. Error bars represent s.e.m.; *t-test, P<0.05. (D) CNIH does not affect the subcellular distribution of TACE. Upper panel: cell surface protein biotinylation followed by avidin precipitation and anti-TACE western blot. Lower panel: immunoflorescence staining of HeLa cells. Transfected CNIH-HA is expressed only in transfected cells, whereas endogenous hTACE is expressed in all cells. Bar, 20 μm. (E) Effect of CNIH on N-glycosylation of TGFα. HeLa cells were transfected to express TGFα with or without CNIH. Cell lysates were treated with N-glycosidase F, and analyzed by SDS-PAGE and western blotting for TGFα. Increased mobility after treatment indicates N-glycosylation prior to treatment. CNIH increases the level of immature TGFα (form 1) without affecting its N-glycosylation. Dividing vertical white lines indicate parts from the same gel (A).

consistent with our previous data, and thereby decreased the generation of TGFα forms previously shown to have complex N-glycosylation (form 2) (Bringman et al., 1987). The immature form of TGFα in the presence of CNIH was susceptible to *N*-glycosidase F, as was TGFα expressed in the absence of CNIH (Fig. 6E). These data indicate that CNIH does not affect the early N-glycosylation steps and are consistent with retention of TGFα in the ER.

Effect of overexpressed Cni on Grk processing

Similar to our experiments in mammalian cells to examine the effect of CNIH on TGFα processing, we assessed the effect of Cni on transport, processing and secretion of Grk in *Drosophila* S2 cells. Grk processing requires two additional transmembrane proteins, the rhomboid protease B-Rho (also known as stem cell tumor), which cleaves Grk inside the membrane, and Star, a transmembrane protein required for transport of Grk from the ER to the Golgi and for its secretion.

S2 cells express endogenous Cni, B-Rho and Star, as assessed by RT-PCR (data not shown). However, the endogenous levels of B-Rho and Star appear insufficient for processing and secretion of ectopically expressed Grk, as detected by immunoblotting. Consistent with published data (Ghiglione et al., 2002), coexpression of Star and B-Rho resulted in processing of the 49 kDa Grk into a cleavage product of 40 kDa (processed Gurken; pGrk) and secretion of this Grk form into the medium (Fig. 7A). This result supports the proposed role of Star as a cargo receptor in transport and of B-Rho in cleavage of Grk (Ghiglione et al., 2002; Guichard et al., 2000; Urban et al., 2002). Processing of both the untagged and the larger Myc-tagged Grk was dependent on coexpression of B-Rho and Star (Fig. 7A,B; data not shown) (Ghiglione et al., 2002).

Next, we studied the effect of Cni expression on the processing of Grk. In the presence of Star and B-Rho, increased Cni levels resulted in reduced levels of processed Grk and increased levels of non-cleaved Grk (Fig. 7B, compare lanes 4 and 3, top panel). These results indicate that, similar to the effect of CNIH on TGFα processing in mammalian cells, ectopic Cni causes an accumulation of transmembrane Grk in its non-

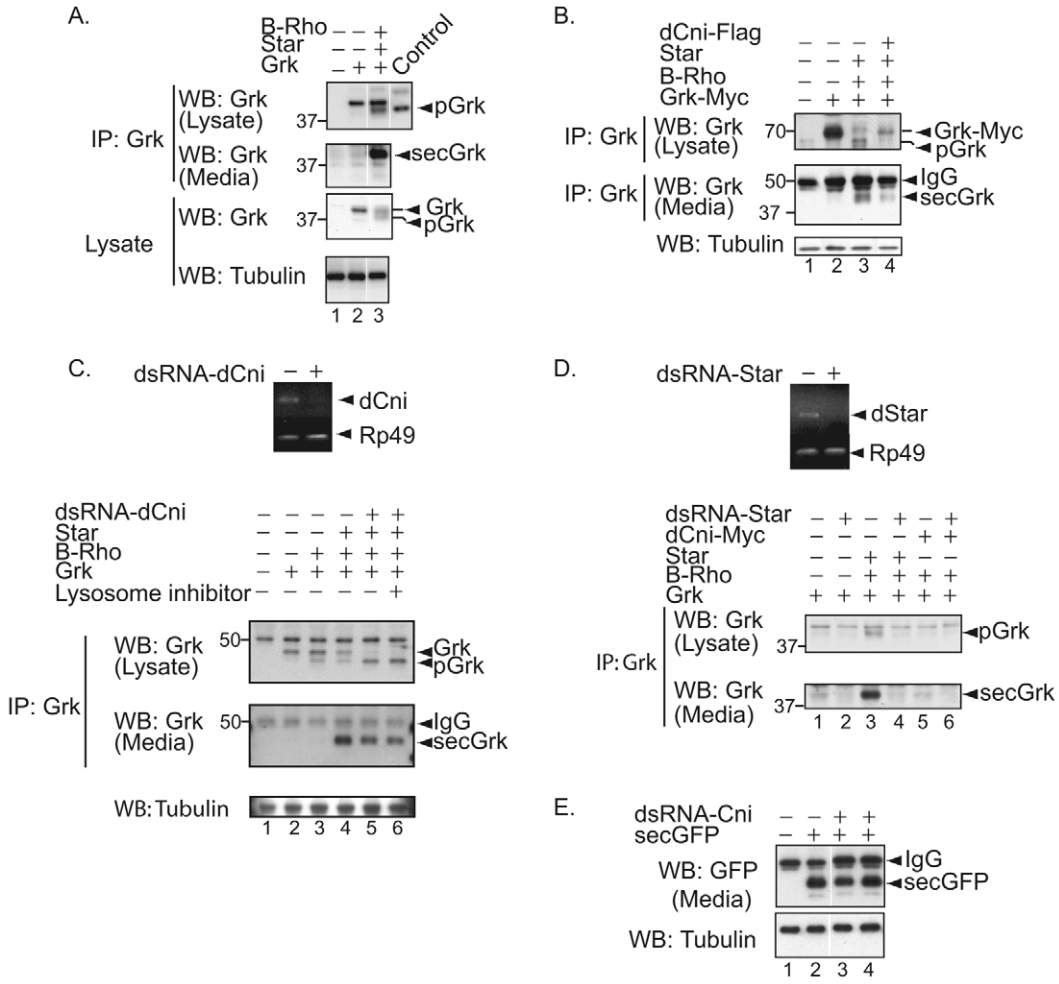

Fig. 7. Role of *Drosophila* Cni (dCni) in Grk processing and secretion. (A) S2 cells were transfected to express Grk, Star, B-Rho and/or a secreted form of Grk (secGrk). Grk expression was visualized by immunoprecipitation and/or blotting with an antibody against the Grk ectodomain. (B) dCni enhanced the level of non-processed Grk. S2 cells were transfected to express Myc-Grk, Star, B-Rho and/or dCni-Flag. Myc-Grk in cell lysates and Grk in the media were visualized using anti-Grk ectodomain antibody. (C) Silencing of dCni in S2 cells causes accumulation of processed Grk (pGrk) in the presence of Star and B-Rho, and reduces Grk secretion. Top panel: downregulation of endogenous dCni mRNA expression by dsRNA-dCni, as assessed by RT-PCR. Lower panel: S2 cells were transfected to express Grk, B-Rho and/or Star, and treated with dsRNA-dCni. Grk expression was visualized, as in B. Accumulation of pGrk with dsRNA-Cni treatment was 2.7 fold and secretion of secGrk was 0.5 fold. Treatment with a lysosome inhibitor (chloroquine; 0.5 mM) does not affect pGrk relative accumulation and secretion. (D) Effect of dsRNA-Star on Grk processing and secretion. Top panel: downregulation of endogenous Star mRNA by dsRNA-Star, assessed by RT-PCR. Lower panels: S2 cells were transfected to express Grk, B-Rho, Star and/or dCni-Myc, and treated with dsRNA targeting Star. Grk was visualized using anti-Grk ectodomain antibody. (E) Silencing of dCni does not affect the general secretory pathway in cells transfected with secretable GFP (Grk-signal peptide-GFP). Dividing vertical white lines indicate parts from the same gel (A,E).

processed form, thereby probably preventing B-Rho-mediated cleavage in the ER (see also in Discussion).

Effect of siRNA-mediated downregulation of Cni expression on Grk processing

To complement the CNIH overexpression experiments, we also examined the effect of CNIH-specific siRNAs on the processing of transmembrane TGFα in mammalian cells. Although we observed a decrease of CNIH mRNA in cells transfected with CNIH siRNA (data not shown), we were unable to verify whether the corresponding CNIH protein level was decreased because of the limited antibody quality. In spite of substantial effort, we were ultimately unable to devise a successful strategy to knock down the expression of all four mammalian cornichon homologs. This lack of success relates to the difficulty in targeting the expression of four closely related gene products that likely exhibit functional redundancy, and in assessing the downregulation of all four cornichon homologs using antibodies against CNIH that presumably crossreact with the other cornichon proteins. Additionally, no successful approach based on dominant-negative interference could be developed using any cornichon deletion mutant (data not shown).

However, we were successful in evaluating the effect of silencing Cni expression in S2 cells, which have only one Cni gene. In S2 cells, as in mammalian cells, Cni and CNIH behaved similarly in retaining EGFR ligands in their immature

forms (see above). Using dsRNA silencing, we effectively reduced the level of Cni mRNA, as determined by RT-PCR (Fig. 7C). Silencing of Cni expression in the presence of B-Rho and Star resulted in increased levels of processed Grk (pGrk), and a reduction of the immature Grk form in the cell lysate (Fig. 7C, lanes 4-6, upper panel). This intracellular accumulation of pGrk is consistent with the increased levels of processed Grk in *Drosophila* oocytes lacking Cni (Bokel et al., 2006) and of Axl2 in Erv14-deficient yeast (Powers and Barlowe, 1998). This effect was not evident when Grk was expressed without B-Rho and Star (data not shown).

Role of Cni in the secretion of soluble Grk

To further evaluate the participation of Cni in Grk transport, we studied the effects of both increased Cni levels and Cni silencing on the secretion of soluble Grk into the medium. These effects were evaluated in cells ectopically expressing B-Rho and Star, since they are required for Grk processing (Fig. 7A,B) (Ghiglione et al., 2002). Silencing of Cni by dsRNA decreased the level of secreted Grk, but with concomitant accumulation of processed Grk (Fig. 7C, compare lanes 4 and 5, middle panel). The absence of Cni does not appear to affect the stability of Grk or processed Grk, as there was no difference in the levels of either form when S2 cells were treated with a lysosome inhibitor (Fig. 7C, compare lane 4 with 5 and 6). Further, the absence of Cni does not appear to alter the general secretory pathway, since dsRNA silencing of Cni did not affect the secretion of soluble GFP (Fig. 7E). These results suggest that the level of Cni impacts the processing and the secretion of Grk.

Effect of siRNA-mediated downregulation of Star on Grk secretion

Star has been proposed to function as a scaffold required for transport of Grk from the ER into the Golgi and for subsequent secretion (Ghiglione et al., 2002; Urban et al., 2002). Analogous to the role of Star, Cni appears to regulate the export of TGFα proteins, or of Axl2 in yeast, from the ER into the Golgi. This analogy raises the question of the relative roles and significance of Star vis-à-vis Cni. As shown using S2 cells (Fig. 7D), both B-Rho and Star are required for processing of Grk and secretion of soluble Grk. Inhibition of Star expression using dsRNA significantly reduced Grk secretion (Fig. 7D, lanes 3 and 4, bottom panel). Overexpression of Cni did not rescue the effect of Star-specific dsRNA on Grk processing and secretion (Fig. 7D, lane 6). Thus, even though the silencing of Star had a similar inhibitory effect on secretion of soluble Grk, both Star and Cni are required for secretion of soluble Grk into the medium.

Discussion

Cornichon was originally identified in *Drosophila*, as inactivation of the gene results in a lack of Grk activity and inability of Grk to stimulate the EGFR (Roth et al., 1995). While this manuscript was in preparation, it was proposed that Cni acts as a cargo receptor for Grk in the ER (Bokel et al., 2006). The Cni-related Erv14 in *S. cerevisiae* has been localized to the ER and is required for polarized transport of Axl2 and bud site selection (Powers and Barlowe, 1998; Powers and Barlowe, 2002). Recently, four genes for Cni-related proteins were identified in vertebrates, indicating the existence of a small family of Cni-related proteins in eukaryotes. No functional studies on vertebrate cornichon proteins have been reported. We have evaluated in parallel the function of *Drosophila* and human cornichon. Our results characterize a role for cornichon proteins in transport and maturation of TGFα family proteins and reveal functional conservation from yeast to mammalian cells.

The NCBI database indicates the existence of four mammalian cornichon paralogs, with the one cloned and characterized in this report corresponding to human CNIH. Human CNIH, CNIH2 and CNIH3 share substantial sequence identity, whereas CNIH4 is divergent. Comparison of the sequences of human CNIH, *Drosophila* Cni and yeast Erv14 reveals a conservation of the predicted three-transmembrane topology and sequence conservation that is highest in the loop between the first and second transmembrane domains and in the third transmembrane region (Powers and Barlowe, 2002).

We examined the subcellular localization of Cni and CNIH. In yeast, Erv14 is localized to the ER and participates in the formation of COPII vesicles through binding to COPII coat subunits (Powers and Barlowe, 2002). Consistent with the localization of Erv14 in yeast, *Drosophila* Cni was recently proposed to localize to the ER of follicular cells (Bokel et al., 2006). We now show by immunofluorescence and electron microscopy that Cni and CNIH are both localized to the ER and cis-Golgi, in S2 and HeLa cells, respectively. Cni colocalized with the ER markers KDEL-GFP in S2 cells and CNIH with calnexin in HeLa cells. Additionally, from immunofluorescence studies Cni was found to colocalized with p120 in S2 cells and CNIH with GM130 in HeLa cells, both markers of Golgi. In HeLa cells, CNIH also partially colocalized with SEC23, a component of the COPII vesicle coat complex that localizes to ER exit sites. CNIH coimmunoprecipitated with GM130 and TGFα-bound GRASP55, both of which are localized in the Golgi. These results suggest that the *Drosophila* and human cornichon proteins cycle between the ER and the Golgi. The similar localization of Erv14, Cni and CNIH to the ER of yeast, *Drosophila* and human cells, respectively, suggests an analogous role for cornichon in these organisms.

Further evidence for a conservation of cornichon function from yeast to mammalian cells was provided by functional rescue experiments in yeast. We found that CNIH expression rescued the bud site selection phenotype in Erv14-deficient cells with similar efficiency as Erv14 itself.

Cni and CNIH both associated with TGFα family proteins, but not with several other transmembrane proteins, such as the transferrin or EGF receptors. Thus, Cni interacted with Grk in S2 cells, whereas CNIH interacted with TGFα and amphiregulin in HeLa cells. Specifically, Cni and CNIH interacted primarily with the immature forms of TGFα family proteins thought to localize to the ER, and much less efficiently with the fully glycosylated or mature processed ligands. We also demonstrate that Cni and CNIH colocalize with Grk and TGFα, respectively, in the ER and cis-Golgi.

It has been shown, using recombinant proteins, that the N-terminal segment of Cni can interact with a segment of Grk (Bokel et al., 2006). Our results extend this observation through mutation and coimmunoprecipitation analyses using lysates from mammalian and *Drosophila* cells. We identified the EGF core, conserved in TGFα and Grk, as essential for the interaction with Cni. This observation may explain the specificity of the physical and functional interactions of Cni proteins with TGFα family proteins, and raises the possibility

that other EGF repeat proteins, such as Notch proteins, may interact with Cni as well. Although these observations illustrate a conserved function of *Drosophila* and human cornichon proteins, Axl2, whose transport requires Erv14, does not have an EGF repeat. Thus, structural ectodomain features that are not obvious by sequence comparison may mediate the interaction with cornichon proteins and extend the selectivity for cornichon interactions.

Our results also provide insight into the mechanism whereby Cni regulates transport of Grk and other TGFα family proteins (Fig. 8). Previous results showed that in the absence Cni, Grk is not transported to the plasma membrane, suggesting a role for Cni as a cargo receptor (Bokel et al., 2006). Our results suggest that cornichon additionally has a retention function, i.e. that it might help retain TGFα family proteins in the ER as a way of regulating transit into the Golgi. Thus, an increase in Cni level results in retention of unprocessed Grk in the ER. Accordingly, increased CNIH levels enhance the levels of immature TGFα and decrease TGFα processing and cell surface presentation. Expression of CNIH in HeLa cells also increased the retention of TGFα, illustrating the conservation of cornichon function between *Drosophila* and mammalian cells. Retention of TGFα in the ER with increased CNIH expression was also apparent by immunofluorescence, showing colocalization of CNIH with increased TGFα staining. The observations that both increased cornichon levels and lack of cornichon result in a retention of immature TGFα family proteins suggest that cornichon is required in stoichiometric amounts. Similarly to cornichon, increased levels and siRNA-mediated downregulation of Sec16, another protein at ER exit sites, also inhibits ER-to-Golgi transport (Watson et al., 2006). We do not know whether the retention of TGFα proteins by increased cornichon levels occurs through inhibition of transport from the ER to the Golgi or by retrograde transport from the Golgi to the ER. However, the regulation of transport by cornichon proteins is likely to involve interaction of cornichon with the COPII complex, as suggested by our electron immunolocalization studies in S2 cells. Although we could not detect an interaction between Cni or CNIH and COPII proteins using a biochemical approach, deletion of the C-terminal cornichon segment, which in yeast interacts with COPII (Powers and Barlowe, 1998), generates a protein that still interacts with TGFα but is defective for retention. We hypothesize that the C-terminal cornichon segment plays a key role in the ability of cornichon to regulate transport by interacting with the COPII complex in yeast, *Drosophila* and mammalian cells. Such conservation of function is consistent with the sequence conservation in that cornichon segment and explains why addition of the C-terminal Cni segment to the cytoplasmic domain of Grk partially rescues the defect in Grk transport in the absence of Cni (Bokel et al., 2006).

The ability of cornichon to regulate the processing of TGFα family proteins also enables it to regulate the secretion of EGFR ligands. Increased cornichon expression inhibited the secretion of TGFα family ligands, Grk in the case of Cni and TGFα or amphiregulin in the case of CNIH. The decrease in the level of ligand secreted into the medium might be explained by decreased ligand processing and thus lower levels of transmembrane ligand that are subject to ectodomain shedding.

To better understand our observations in S2 cells, other components involved in Grk processing, such as Star and B-Rho, need to be considered. Star was shown to bring Grk from the ER to the Golgi and is involved in Grk secretion (Ghiglione et al., 2002; Urban and Freeman, 2002). It was also shown that Grk is cleaved by B-Rho, but whether this occurs in the ER, the Golgi or in between is a matter of debate (Ghiglione et al., 2002; Tsruya et al., 2002). Our results strongly suggest that Grk processing occurs in the ER. Like Star, Cni has been proposed to function as a cargo receptor for Grk (Bokel et al., 2006). Although their sequences are different, Star and Cni both require the ectodomain of TGFα-like ligands for binding (Bokel et al., 2006; Tsruya et al., 2002). However, Cni does not complement the absence of Star or vice versa.

In an effort to integrate our data with what has been reported about Grk processing and secretion, we envisage the following model (Fig. 8). Cni interacts with Grk in the ER and brings it to COPII vesicles at ER exit sites, where Grk may come into contact with Star. Cni travels with Grk and Star to the Golgi, but returns to the ER. Grk continues through the pathway with Star to allow transport to the plasma membrane and secretion. This model accommodates both our results and those reported elsewhere. First, when Cni expression is knocked down, we expect accumulation of processed Grk because Cni is not present to regulate its transport to the Golgi. It is possible that

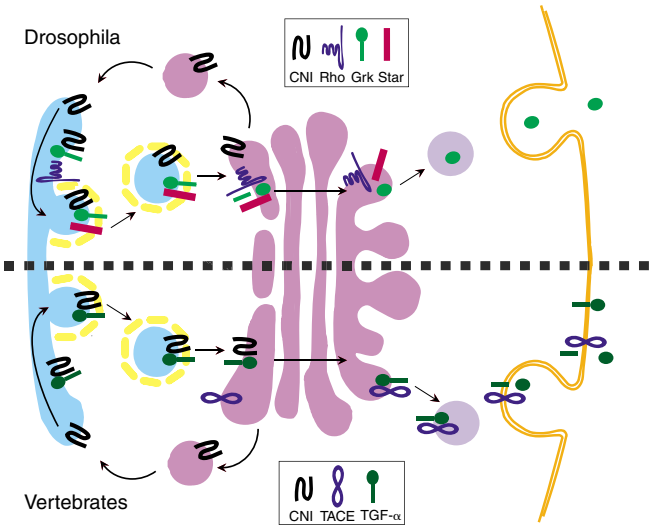

Fig. 8. Schematic representation of the model of cornichon action in transport of TGFα family proteins. In both *Drosophila* and vertebrates, cornichon interacts in the ER with TGFα family proteins, such as Grk in *Drosophila* and TGFα in mammals, and controls and is required for their transport from the ER into the Golgi. In *Drosophila*, Star and Rhomboid control the transport and cleavage of Grk to the cell surface. The late endosomal compartment that may be important for the activities of Rhomboid and Star is not shown. In vertebrates, no roles for Rhomboid or Star homologs in the transport or cleavage of TGFα family proteins have been characterized. Instead, the transmembrane metalloprotease TACE is known to cleave TGFα to release the soluble ectodomain, and this may primarily occur late during transport and at the cell surface. Other ADAM proteases may control the ectodomain release of other TGFα family proteins. The precise localization of proteins and timing of cleavage of TGFα remains to be better characterized and, as shown, is not meant to be definitive.

the increase in processing could be due to unhindered access of B-Rho to Grk when Cni is not present. Thus, although Grk is processed, Cni is required for further transit and its absence results in the inability of Grk to be secreted efficiently, even in the presence of Star. Second, when Cni is in excess, Cni might not release Grk in the Golgi or not allow Star to bind, resulting in Grk returning to the ER with Cni. Excess Cni may also prevent Grk cleavage by B-Rho by preventing interaction of Grk with B-Rho in the ER. Third, when Star expression is knocked down, Cni can bring Grk into COPII vesicles for transport to the Golgi, but, without Star, Grk cannot proceed through the pathway. Further, in the absence of Star, Grk cleavage is inhibited, possibly because Grk remains bound to Cni and access of B-Rho is denied. Thus, Cni and Star are both needed for the transport and secretion of Grk. The elucidation of the precise role of each requires further investigation.

Materials and Methods

Complementation assays

pRS316-Erv14 and pRS316-Erv14-HA were described previously (Powers and Barlowe, 1998). A yeast plasmid to express human HA-tagged CNIH was made by subcloning the coding sequence of CNIH from pRK5 into pRS316. The yeast strain BY4741 MATα his3D1 leu2D0 lys2D0 ura3D0 (Brachmann et al., 1998) was disrupted at the Erv14 locus by inserting the kanamycin gene to create the Δerv14 strain.

Complementation assays were done as described previously (Powers and Barlowe, 1998). Cells with six or more bud scars were examined for axial or non-axial budding.

Cell culture and transfections

CHO, and Cα cells [CHO derivatives that expresses TGFα (Shum et al., 1994)], were grown in F-12 Ham's nutrient mix medium (Gibco-BRL). The medium for Cα cells was supplemented with 400 μg/ml geneticin (Gibco-BRL). HeLa, 293T and HCA-7 cells were grown in DMEM-21 with 4.5 g/l glucose (Gibco-BRL). Medium were supplemented with 10% FBS (Gibco-BRL), 100 U/ml penicillin and 100 μg/ml streptomycin. S2 cells were grown in Schields and Sang M3 medium with 10% FBS at 27°C. Cells were transfected in six-well plates with Fugene 6 (Roche) or Lipofectamine LTX (Invitrogen). Transfection efficiency was evaluated using parallel wells transfected with an EGFP plasmid.

Expression plasmids

The coding sequence for CNIH was obtained from HeLa cells using RT-PCR based on the *Drosophila* Cni sequence (Roth et al., 1995). To express C-terminally tagged CNIH in mammalian cells, the CNIH sequence was cloned into *Eco*RI-*Sal*I-linearized pRK5M, pRK5F (Feng et al., 1995) or pRK5HA (Feng et al., 1998), to express Myc-, Flag- and HA-tagged CNIH, respectively. An expression plasmid for N-terminally Myc-tagged CNIH was made by subcloning the CNIH sequence into *Eco*RI-*Sal*I-linearized pXF-myc. To express *Drosophila* Cni in mammalian cells, the Cni sequence was inserted into *Eco*RI-*Sal*I-linearized pMT and pAc 5.1 (Invitrogen) or into *Eco*RI-linearized pRK5M and pRK5F.

The plasmids pRK7-TGFα, pRK7-TGFαΔC and pRK-TGFαΔE have been described previously (Shi et al., 2000; Shum et al., 1994). Expression plasmids for amphiregulin (pRK5-AR-Flag) or GM130 (pRK5-GM130-Myc) were made by subcloning the coding sequences into pRK5F or pRK5M (Feng et al., 1998). Plasmid pRK5-p59 to express GRASP55 has been described previously (Kuo et al., 2000). C-terminally Myc-tagged Star, GFP-fused B-Rho (BRho-GFP; B-Rho is also known as Rho – FlyBase), C-terminally tagged Grk and soluble Grk (secGrk) were expressed as described previously (Ghiglione et al., 2002). The pUAST vector expressing Grk has been described elsewhere (Queenan et al., 1999). Plasmids encoding AP-tagged TGFα or amphiregulin (Sahin et al., 2004) were provided by S. Higashiyama and C. Blobel (Sloan-Kettering Institute, NY).

Antibodies

Rabbit antiserum against CNIH was raised against the peptide DELKTDYKNPIDQCN (CNIH residues 32-46) (SynPep, Dublin, CA). IgG was purified using the Melon Gel IgG Spin Purification Kit (Pierce, IL, USA). Mouse anti-Flag, anti-Myc and anti-HA, and rabbit anti-Flag and anti-Myc were from Sigma. The anti-HA rat monoclonal antibody was from Roche. The anti-TGFα monoclonal antibody Ab-1 was from Oncogene Sciences (Cambridge, MA). Anti-calnexin was from Stressgen (Victoria, BC, Canada) and anti-GM130 monoclonal antibody was from Transduction Laboratories. Grk was detected using the 1D12 antibody (Developmental Studies Hybridoma Bank). Sec23 (dSec23p) was detected using a rabbit antibody (Affinity BioReagents, Golden, CO).

Coimmunoprecipitation, cell surface biotin labeling and *N*-glycosidase F treatment

Cells were lysed in TBS-EDTA with 1% Triton X-100 and protease inhibitor cocktail (Roche). For immunoprecipitation, the lysate was precleared with protein G beads (Roche) and incubated with antibody for 2 hours to overnight at 4°C. After four 5-minute washes with lysis buffer, the samples were separated by SDS-PAGE, blotted onto Immobilon-P PVDF membrane (Millipore) and probed with antibody.

Cell surface biotin labeling was done as described previously (Kuo et al., 2000). For deglycosylation, lysates were treated with 1 mU of *N*-glycosidase F (New England Biolabs) for 1 hour at 37°C.

RNA interference

dsRNA was generated as described previously (Clemens et al., 2000). Cni and Star cDNAs with flanking T7 RNA polymerase sites were generated by RT-PCR from S2 cells using primers: Cni, 5′-TAATACGACTCACTATAGGGCGTGCTCCAGC-GATTTTACAAG-3′ (forward), 5′-GAGATCCCCAGGCAAGAGCTTG-3′ (reverse); Star, 5′-TAATACGACTCACTATAGGGAGGAGTCATGTCGCAGC-3′ (forward), 5′-GTGGTGCTGTCTGTGCG-3′ (reverse). The T7 templates were purified and used for dsRNA synthesis using the MEGASCRIPT T7 kit (Ambion). DsRNAi (20-30 μg) was added to 1×10^6 cells/well (six well-plates) in M3 serum-free medium (Sigma).

Grk cleavage in S2 cells

Grk cleavage in S2 cells was assayed as described previously (Ghiglione et al., 2002). After centrifugation at 16,000 ***g*** at 4°C, supernatants were subjected to immunoprecipitation, followed by SDS-PAGE and immunoblotting (Kuo et al., 2000; Shi et al., 2000).

Shedding assay

The shedding assay, using alkaline phosphatase (AP)-fused TGFα family proteins, has been described previously (Sahin et al., 2004; Zheng et al., 2002). Briefly, the day after transfection, cells were starved for 1 hour before adding medium with or without 25 ng/ml PMA (phorbol 12-myristate 13-acetate; Sigma). Conditioned media were collected after 1 hour and assayed for AP activity (Sahin et al., 2004).

Microscopy

Transfected HeLa and Cα cells were fixed with cold methanol-acetone for 3 minutes (Nakagawa et al., 2005) and incubated with antibody in blocking solution for 1 hour at 37°C. After four 5-minute washes with PBS, cells were incubated in a 1:500 dilution of Rhodamine- or FITC-conjugated secondary antibody (Jackson ImmunoResearch) in blocking solution at room temperature. S2 cells were fixed for 10 minutes in 3% PFA in PBS at room temperature, permeabilized with Triton X-100 and processed for immunofluorescence. Cells were observed by epifluorescence and confocal microscopy as described previously (Nakagawa et al., 2005).

Immunoelectron microscopy was done as described by McCaffery and Farquhar (McCaffery and Farquhar, 1995) using a Philips Tecnai 10 electron microscope. ER membranes were identified based on structure and morphology (Kondylis and Rabouille, 2003). S2 cells not expressing tagged-Cni were used to confirm non-specific background. More than 100 gold particles were counted and classified for the different membrane categories. The results are expressed in percentages of the total labeling (Table 1).

Images, saved as 12 bit TIFF files, were quantitatively analyzed using ImageJ software (http://rsb.info.nih.gov/ij/). Microsoft Excel was used for simple data analyses.

We thank T. Shupbach, C. Rabouille, N. Perrimon, E. Bach, E. Arzt and J. Huang for plasmids. We thank R. Vale for the KDEL-GFP S2 cell line. We are grateful to G. Pesce for help with the yeast experiments, K. Kobayashi for critically reading the manuscript and J. Engel and I. Hsieh for support with electron microscopy. We acknowledge the use of Flybase. This project was supported by NIH R01 grant CA54826 to R.D., a Pew Trust Latin American Fellowship to C.P.C. and an NIH training grant to the Cardiovascular Research Institute for D.P.

References

Bokel, C., Dass, S., Wilsch-Brauninger, M. and Roth, S. (2006). *Drosophila* Cornichon acts as cargo receptor for ER export of the TGFα-like growth factor Gurken. *Development* **133**, 459-470.

Brachmann, C. B., Davies, A., Cost, G. J., Caputo, E., Li, J., Hieter, P. and Boeke, J. D. (1998). Designer deletion strains derived from Saccharomyces cerevisiae S288C: a useful set of strains and plasmids for PCR-mediated gene disruption and other applications. *Yeast* **14**, 115-132.

Brachmann, R., Lindquist, P. B., Nagashima, M., Kohr, W., Lipari, T., Napier, M. and Derynck, R. (1989). Transmembrane TGFα precursors activate EGF/TGFα receptors. *Cell* **56**, 691-700.

Bringman, T. S., Lindquist, P. B. and Derynck, R. (1987). Different transforming growth factor-alpha species are derived from a glycosylated and palmitoylated transmembrane precursor. *Cell* **48**, 429-440.

Brown, C. L., Meise, K. S., Plowman, G. D., Coffey, R. J. and Dempsey, P. J. (1998). Cell surface ectodomain cleavage of human amphiregulin precursor is sensitive to a metalloprotease inhibitor. Release of a predominant N-glycosylated 43-kDa soluble form. *J. Biol. Chem.* **273**, 17258-17268.

Clemens, J. C., Worby, C. A., Simonson-Leff, N., Muda, M., Maehama, T., Hemmings, B. A. and Dixon, J. E. (2000). Use of double-stranded RNA interference in *Drosophila* cell lines to dissect signal transduction pathways. *Proc. Natl. Acad. Sci. USA* **97**, 6499-6503.

Derynck, R. (1992). The physiology of transforming growth factor-alpha. *Adv. Cancer Res.* **58**, 27-52.

Fan, H. and Derynck, R. (1999). Ectodomain shedding of TGFα and other transmembrane proteins is induced by receptor tyrosine kinase activation and MAP kinase signaling cascades. *EMBO J.* **18**, 6962-6972.

Feng, X. H., Filvaroff, E. H. and Derynck, R. (1995). Transforming growth factor-beta (TGFβ)-induced down-regulation of cyclin A expression requires a functional TGFβ receptor complex. Characterization of chimeric and truncated type I and type II receptors. *J. Biol. Chem.* **270**, 24237-24245.

Feng, X. H., Zhang, Y., Wu, R. Y. and Derynck, R. (1998). The tumor suppressor Smad4/DPC4 and transcriptional adaptor CBP/p300 are coactivators for smad3 in TGFβ-induced transcriptional activation. *Genes Dev.* **12**, 2153-2163.

Ghiglione, C., Bach, E. A., Paraiso, Y., Carraway, K. L., 3rd, Noselli, S. and Perrimon, N. (2002). Mechanism of activation of the *Drosophila* EGF receptor by the TGFα ligand Gurken during oogenesis. *Development* **129**, 175-186.

Guichard, A., Roark, M., Ronshaugen, M. and Bier, E. (2000). brother of rhomboid, a rhomboid-related gene expressed during early *Drosophila* oogenesis, promotes EGF-R/MAPK signaling. *Dev. Biol.* **226**, 255-266.

Hopper, N. A., Lee, J. and Sternberg, P. W. (2000). ARK-1 inhibits EGFR signaling in C. elegans. *Mol. Cell* **6**, 65-75.

Kondylis, V. and Rabouille, C. (2003). A novel role for dp115 in the organization of tER sites in *Drosophila*. *J. Cell Biol.* **162**, 185-198.

Kuo, A., Zhong, C., Lane, W. S. and Derynck, R. (2000). Transmembrane transforming growth factor-alpha tethers to the PDZ domain-containing, Golgi membrane-associated protein p59/GRASP55. *EMBO J.* **19**, 6427-6439.

Lee, D. C., Fenton, S. E., Berkowitz, E. A. and Hissong, M. A. (1995). Transforming growth factor alpha: expression, regulation, and biological activities. *Pharmacol. Rev.* **47**, 51-85.

Massague, J. and Pandiella, A. (1993). Membrane-anchored growth factors. *Annu. Rev. Biochem.* **62**, 515-541.

McCaffery, J. M. and Farquhar, M. G. (1995). Localization of GTPases by indirect immunofluorescence and immunoelectron microscopy. *Meth. Enzymol.* **257**, 259-279.

Nakagawa, T., Guichard, A., Castro, C. P., Xiao, Y., Rizen, M., Zhang, H. Z., Hu, D., Bang, A., Helms, J., Bier, E. et al. (2005). Characterization of a human rhomboid homolog, p100hRho/RHBDF1, which interacts with TGFα family ligands. *Dev. Dyn.* **233**, 1315-1331.

Neuman-Silberberg, F. S. and Schupbach, T. (1996). The *Drosophila* TGFalpha-like protein Gurken: expression and cellular localization during *Drosophila* oogenesis. *Mech. Dev.* **59**, 105-113.

Perrimon, N. and Perkins, L. A. (1997). There must be 50 ways to rule the signal: the case of the *Drosophila* EGF receptor. *Cell* **89**, 13-16.

Powers, J. and Barlowe, C. (1998). Transport of axl2p depends on erv14p, an ER-vesicle protein related to the *Drosophila* cornichon gene product. *J. Cell Biol.* **142**, 1209-1222.

Powers, J. and Barlowe, C. (2002). Erv14p directs a transmembrane secretory protein into COPII-coated transport vesicles. *Mol. Biol. Cell* **13**, 880-891.

Queenan, A. M., Barcelo, G., Van Buskirk, C. and Schupbach, T. (1999). The transmembrane region of Gurken is not required for biological activity, but is necessary for transport to the oocyte membrane in *Drosophila*. *Mech. Dev.* **89**, 35-42.

Ray, R. P. and Schupbach, T. (1996). Intercellular signaling and the polarization of body axes during *Drosophila* oogenesis. *Genes Dev.* **10**, 1711-1723.

Roth, S., Neuman-Silberberg, F. S., Barcelo, G. and Schupbach, T. (1995). cornichon and the EGF receptor signaling process are necessary for both anterior-posterior and dorsal-ventral pattern formation in *Drosophila*. *Cell* **81**, 967-978.

Sahin, U., Weskamp, G., Kelly, K., Zhou, H. M., Higashiyama, S., Peschon, J., Hartmann, D., Saftig, P. and Blobel, C. P. (2004). Distinct roles for ADAM10 and ADAM17 in ectodomain shedding of six EGFR ligands. *J. Cell Biol.* **164**, 769-779.

Schlessinger, J. (2002). Ligand-induced, receptor-mediated dimerization and activation of EGF receptor. *Cell* **110**, 669-672.

Schweitzer, R., Shaharabany, M., Seger, R. and Shilo, B. Z. (1995). Secreted Spitz triggers the DER signaling pathway and is a limiting component in embryonic ventral ectoderm determination. *Genes Dev.* **9**, 1518-1529.

Shi, W., Fan, H., Shum, L. and Derynck, R. (2000). The tetraspanin CD9 associates with transmembrane TGFα and regulates TGFα-induced EGF receptor activation and cell proliferation. *J. Cell Biol.* **148**, 591-602.

Shilo, B. Z. (2005). Regulating the dynamics of EGF receptor signaling in space and time. *Development* **132**, 4017-4027.

Shum, L., Reeves, S. A., Kuo, A. C., Fromer, E. S. and Derynck, R. (1994). Association of the transmembrane TGFα precursor with a protein kinase complex. *J. Cell Biol.* **125**, 903-916.

Sunnarborg, S. W., Hinkle, C. L., Stevenson, M., Russell, W. E., Raska, C. S., Peschon, J. J., Castner, B. J., Gerhart, M. J., Paxton, R. J., Black, R. A. et al. (2002). Tumor necrosis factor-alpha converting enzyme (TACE) regulates epidermal growth factor receptor ligand availability. *J. Biol. Chem.* **277**, 12838-12845.

Tsruya, R., Schlesinger, A., Reich, A., Gabay, L., Sapir, A. and Shilo, B. Z. (2002). Intracellular trafficking by Star regulates cleavage of the *Drosophila* EGF receptor ligand Spitz. *Genes Dev.* **16**, 222-234.

Urban, S. and Freeman, M. (2002). Intramembrane protelysis controls diverse signalling pathways throughout evolution. *Curr. Opin. Genet. Dev.* **12**, 512-518.

Urban, S., Lee, J. R. and Freeman, M. (2002). A family of Rhomboid intramembrane proteases activates all *Drosophila* membrane-tethered EGF ligands. *EMBO J.* **21**, 4277-4286.

Utku, N., Bulwin, G. C., Beinke, S., Heinemann, T., Beato, F., Randall, J., Schnieders, B., Sandhoff, K., Volk, H. D., Milford, E. et al. (1999). The human homolog of *Drosophila* cornichon protein is differentially expressed in alloactivated T-cells. *Biochim. Biophys. Acta* **1449**, 203-210.

Watson, P., Towney, A. K., Koka, P., Palmer, K. J. and Stephens, D. J. (2006). Sec16 defines endoplasmic reticulum exit sites and is required for secretory cargo export in mammalian cells. *Traffic* **7**, 1678-1687.

Zheng, Y., Schlondorff, J. and Blobel, C. P. (2002). Evidence for regulation of the tumor necrosis factor alpha-convertase (TACE) by protein-tyrosine phosphatase PTPH1. *J. Biol. Chem.* **277**, 42463-42470.